Spin-3 Chromium Bose-Einstein Condensates

L. Santos[1] and T. Pfau[2]

[1]*Institut für Theoretische Physik III, Universität Stuttgart, Pfaffenwaldring 57 V, D-70550 Stuttgart, Germany*
[2]*5. Physikalisches Institut, Universität Stuttgart, Pfaffenwaldring 57 V, D-70550 Stuttgart, Germany*
(Received 28 October 2005; revised manuscript received 15 December 2005; published 16 May 2006)

We analyze the physics of spin-3 Bose-Einstein condensates, and, in particular, the new physics expected in ongoing experiments with condensates of chromium atoms. We first discuss the ground-state properties, which, depending on still unknown chromium parameters, and for low magnetic fields, can present various types of phases. We also discuss the spinor dynamics in chromium spinor condensates, which present significant qualitative differences when compared to other spinor condensates. In particular, dipole-induced spin relaxation may lead for low magnetic fields to transfer of spin into angular momentum similar to the well-known Einstein-de Haas effect. Additionally, a rapid large transference of population between distant magnetic states also becomes possible.

DOI: 10.1103/PhysRevLett.96.190404 PACS numbers: 03.75.Mn, 03.75.Hh, 03.75.Kk

Within the very active field of ultracold atomic gases, multicomponent (spinor) Bose-Einstein condensates (BECs) have recently attracted a rapidly growing attention. Numerous works have addressed the rich variety of phenomena revealed by spinor BEC, in particular, in what concerns ground-state and spin dynamics [1–17]. The first experiments on spinor BEC were performed at JILA using mixtures of ^{87}Rb BEC in two magnetically confined internal states (spin-1/2 BEC) [9]. Optical trapping of spinor condensates was first realized in spin-1 sodium BEC at MIT [10] constituting a major breakthrough since, whereas magnetic trapping confines the BEC to weak-seeking magnetic states, an optical trap enables confinement of all magnetic substates. In addition, the atoms in a magnetic substate can be converted into atoms in other substates through interatomic interactions. Hence, these experiments paved the way towards the above mentioned fascinating phenomenology originating from the spin degree of freedom. Various experiments have been realized since then in spin-1 BEC, in particular, in ^{87}Rb in the $F = 1$ manifold. It has been predicted that spin-1 BEC can present just two different ground-state phases, either ferromagnetic or polar [1]. In the case of $F = 1$ ^{87}Rb it has been shown that the ground state presents a ferromagnetic behavior [12,13,18]. These analyses have been recently extended to spin-2 BEC, which presents an even richer variety of possible ground states, including, in addition, the so-called cyclic phases [4,5]. Recent experiments have shown a behavior compatible with a polar ground state, although in the very vicinity of the cyclic phase [12,18]. Recently, spin dynamics has attracted a major interest, revealing the fascinating physics of the coherent oscillations between the different components of the manifold [11–16].

Very recently, a chromium BEC (Cr-BEC) has been achieved at Stuttgart University [19]. Cr-BEC presents fascinating new features when compared to other experiments in BEC. On one hand, since the ground state of ^{52}Cr is $^7S_3$, Cr-BEC constitutes the first accessible example of a spin-3 BEC. We show below that this fact may have very important consequences for both the ground state and the dynamics of spinor Cr-BEC. On the other hand, when aligned into the state with magnetic quantum number $m = \pm 3$, ^{52}Cr presents a magnetic moment $\mu = 6\mu_B$, where μ_B is the Bohr magneton. This dipolar moment should be compared to alkali-metal atoms, which have a maximum magnetic moment of $1\mu_B$, and hence 36 times smaller dipole-dipole interactions. Ultracold dipolar gases have attracted a rapidly growing attention, in particular, in what concerns its stability and excitations [20]. The interplay of the dipole-dipole interaction and spinor-BEC physics has been also considered [6,7]. Recently, the dipolar effects have been observed for the first time in the expansion of a Cr-BEC [21].

This Letter analyzes spin-3 BEC, and, in particular, the new physics expected in ongoing experiments in Cr-BEC. After deriving the equations that describe this system, we focus on the ground state, using single-mode approximation (SMA), showing that various phases are possible, depending on the applied magnetic field, and the (still unknown) value of the s-wave scattering length for the channel of total spin zero. This phase diagram presents small differences in its final form with respect to the diagram first worked out recently by Diener and Ho [22]. In the second part of this Letter, we discuss the spinor dynamics, departing from the SMA. The double nature of Cr-BEC as a spin-3 BEC and a dipolar BEC is shown to lead to significant qualitative differences when compared to other spinor BECs. The larger spin can allow for fast population transfer from $m = 0$ to $m = \pm 3$ without a sequential dynamics as in $F = 2$ ^{87}Rb [12]. In addition, dipolar relaxation violates spin conservation, leading to rotation of the different components, resembling the well-known Einstein-de Haas (EdH) effect [23].

In the following we consider an optically trapped Cr-BEC with N particles. The Hamiltonian regulating Cr-BEC is of the form $\hat{H} = \hat{H}_0 + \hat{V}_{sr} + \hat{V}_{dd}$. The single-particle part of the Hamiltonian, $\hat{H}_0$, includes the trapping energy and the linear Zeeman effect (quadratic Zeeman effect is absent in Cr-BEC), being of the form

$$\hat{H}_0 = \int d\mathbf{r} \sum_m \hat{\psi}_m^\dagger(\mathbf{r}) \left[\frac{-\hbar^2}{2M} \nabla^2 + U_{\rm trap}(\mathbf{r}) + pm \right] \hat{\psi}_m(\mathbf{r}), \quad (1)$$

where $\hat{\psi}_m^\dagger$ ($\hat{\psi}_m$) is the creation (annihilation) operator in the m state, M is the atomic mass, and $p = g\mu_B B$, with $g = 2$ for ^{52}Cr, and B is the applied magnetic field.

The short-range (van der Waals) interactions are given by $\hat{V}_{\rm sr}$. For any interacting pair with spins $\mathbf{S}_{1,2}$, $\hat{V}_{\rm sr}$ conserves the total spin, S, and is thus described in terms of the projector operators on different total spins $\hat{\mathcal{P}}_S$, where $S = 0$, 2, 4, and 6 (only even S is allowed) [1]

$$\hat{V}_{\rm sr} = \frac{1}{2} \int d\mathbf{r} \sum_{S=0}^{6} g_S \hat{\mathcal{P}}_S(\mathbf{r}), \quad (2)$$

where $g_S = 4\pi\hbar^2 a_S/M$, and a_S is the s-wave scattering length for a total spin S. Since $\mathbf{S}_1 \cdot \mathbf{S}_2 = (S^2 - S_1^2 - S_2^2)/2$, then $\sum_S \hat{\mathcal{P}}_S(\mathbf{r}) =: \hat{n}^2(\mathbf{r}):$, $\sum_S \lambda_S \hat{\mathcal{P}}_S(\mathbf{r}) =: \hat{F}^2(\mathbf{r}):$, and $\sum_S \lambda_S^2 \hat{\mathcal{P}}_S(\mathbf{r}) =: \hat{O}^2(\mathbf{r}):$, where :: denotes normal order, $\lambda_S = [S(S+1) - 24]/2$, $\hat{n}(\mathbf{r}) = \sum_m \hat{\psi}_m^\dagger(\mathbf{r})\hat{\psi}_m(\mathbf{r})$, $\hat{F}^2 = \sum_{i=x,y,z} \hat{F}_i^2$, with $\hat{F}_i(\mathbf{r}) = \sum_{mn} \hat{\psi}_m^\dagger(\mathbf{r}) S^i_{mn} \hat{\psi}_n(\mathbf{r})$, and $\hat{O}^2 = \sum_{i,j} \hat{O}_{ij}^2$, with $\hat{O}_{ij} = \sum_{m,n} \hat{\psi}_m^\dagger(\mathbf{r})(S^iS^j)_{mn}\hat{\psi}_n(\vec{r})$. $S^{x,y,z}$ are the spin matrices. Hence,

$$\hat{V}_{\rm sr} = \frac{1}{2} \int d\mathbf{r} [c_0 \colon \hat{n}^2(\mathbf{r}) + c_1 \hat{F}^2(\mathbf{r}) + c_2 \hat{\mathcal{P}}_0(\mathbf{r}) + c_3 \hat{O}^2(\mathbf{r}) \colon], \quad (3)$$

where $\hat{\mathcal{P}}_0(\mathbf{r}) = \frac{1}{7}\sum_{m,n}(-1)^{m+n}\hat{\psi}_m^\dagger \hat{\psi}_{-m}^\dagger \hat{\psi}_n \hat{\psi}_{-n}$, and $c_0 = (-11g_2 + 81g_4 + 7g_6)/77$, $c_1 = (g_6 - g_2)/18$, $c_2 = g_0 + (-55g_2 + 27g_4 - 5g_6)/33$, $c_3 = g_2/126 - g_4/77 + g_6/198$. For the case of ^{52}Cr [24], $a_6 = 112a_B$, where a_B is the Bohr radius, and $c_0 = 0.65g_6$, $c_1 = 0.059g_6$, $c_2 = g0 + 0.374g_6$, and $c_3 = -0.002g_6$. The value of a_0 is unknown, and hence, in the following, we consider different scenarios depending on the value of g_0/g_6. Note that Eq. (3) is similar to that obtained for spin-2 BEC [4,5], the main new feature being the c_3 term, which introduces qualitatively new physics as discussed below.

The dipole-dipole interaction $\hat{V}_{\rm dd}$ is of the form

$$\hat{V}_{\rm dd} = \frac{c_d}{2} \int d\mathbf{r} \int d\mathbf{r}' \frac{1}{|\mathbf{r} - \mathbf{r}'|^3} \hat{\psi}_m^\dagger(\mathbf{r}) \hat{\psi}_{m'}^\dagger(\mathbf{r}') \times [\mathbf{S}_{mn} \cdot \mathbf{S}_{m'n'} - 3(\mathbf{S}_{mn} \cdot \mathbf{e})(\mathbf{S}_{m'n'} \cdot \mathbf{e})] \hat{\psi}_n(\mathbf{r}) \hat{\psi}_{n'}(\mathbf{r}'), \quad (4)$$

where $c_d = \mu_0 \mu_B^2 g_S^2/4\pi$, with μ_0 the magnetic permeability of vacuum, and $\mathbf{e} = (\mathbf{r} - \mathbf{r}')/|\mathbf{r} - \mathbf{r}'|$. For ^{52}Cr $c_d = 0.004g_6$. $\vec{V}_{\rm dd}$ may be rewritten as

$$\hat{V}_{\rm dd} = \sqrt{\frac{3\pi}{10}} c_d \iint \frac{d\mathbf{r} d\mathbf{r}'}{|\mathbf{r} - \mathbf{r}'|^3} \colon \{\mathcal{F}_{zz}(\mathbf{r},\mathbf{r}')Y_{20} + \mathcal{F}_{z,-}(\mathbf{r},\mathbf{r}')Y_{21} + \mathcal{F}_{z,+}(\mathbf{r},\mathbf{r}')Y_{2-1} + \mathcal{F}_{-,-}(\mathbf{r},\mathbf{r}')Y_{22} + \mathcal{F}_{+,+}(\mathbf{r},\mathbf{r}')Y_{2-2}\} \colon, \quad (5)$$

where $\mathcal{F}_{zz}(\mathbf{r},\mathbf{r}') = \sqrt{2/3}[3\hat{F}_z(\mathbf{r})\hat{F}_z(\mathbf{r}') - \hat{\mathbf{F}}(\mathbf{r}) \cdot \hat{\mathbf{F}}(\mathbf{r}')]$, $\mathcal{F}_{z,\pm}(\mathbf{r},\mathbf{r}') = \pm[\hat{F}_\pm(\mathbf{r})\hat{F}_z(\mathbf{r}') + \hat{F}_z(\mathbf{r})\hat{F}_\pm(\mathbf{r}')]$, $\mathcal{F}_{\pm,\pm}(\mathbf{r},\mathbf{r}') = \hat{F}_\pm(\mathbf{r})\hat{F}_\pm(\mathbf{r}')$, $\hat{F}_\pm = \hat{F}_x \pm i\hat{F}_y$, and $Y_{2m}(\mathbf{r} - \mathbf{r}')$ are the spherical harmonics. Note that contrary to the short-range interactions, $\hat{V}_{\rm dd}$ does not conserve the total spin, and may induce a transference of angular momentum into the center of mass (c.m.) degrees of freedom.

We first discuss the ground-state of the spin-3 BEC for different values of g_0, and the magnetic field, p. We consider mean-field (MF) approximation $\hat{\psi}_m(\mathbf{r}) \simeq \sqrt{N}\psi_m(\mathbf{r})$. In order to simplify the analysis of the possible ground-state solutions we perform SMA: $\psi_m(\mathbf{r}) = \Phi(\mathbf{r})\psi_m$, with $\int d\mathbf{r}|\Phi(\mathbf{r})|^2 = 1$. Apart from spin-independent terms the energy per particle is of the form:

$$E = pf_z + \frac{Nc_1\beta}{2}(f_z^2 + f_+f_-) + \frac{2c_2N\beta}{7}|s_-|^2 + \frac{Nc_3\beta}{2}\sum_{ij} O_{ij}^2 + \sqrt{\frac{3\pi}{10}} Nc_d[\sqrt{2/3}\Gamma_0(2f_z^2 - f_+f_-) - 2\Gamma_{+1}f_zf_- + 2\Gamma_{-1}f_zf_+ + \Gamma_{+2}f_-^2 + \Gamma_{-2}f_+^2], \quad (6)$$

where $\beta = \int d\mathbf{r}|\Phi(\mathbf{r})|^4$, $s_- = \frac{1}{2}\sum_m(-1)^m\psi_m\psi_{-m}$, $f_i = \sum_{m,n}\psi_m^* S^i_{mn}\psi_n$, $O_{ij} = \sum_{m,n}\psi_m^*(S^iS^j)_{mn}\psi_n$, and $\Gamma_m = \int d\mathbf{r} \int d\mathbf{r}' |\Phi(\mathbf{r}')|^2 |\Phi(\mathbf{r})|^2 Y_{2m}(\mathbf{r} - \mathbf{r}')/|\mathbf{r} - \mathbf{r}'|^3$. Note that $\Gamma_{\pm 1} = 0$ for any symmetric density $|\Phi(\mathbf{r})|^2$.

Let us consider a magnetic field in the z direction. Hence, the ground-state magnetization must be aligned with the external field, and $f_+ = f_- = 0$. Then, we obtain that $\sum_{ij} O_{ij}^2 = 77 - 12\gamma_z + 3\gamma_z^2/2 - f_z^2/2 + |\eta|^2/2 + 2|\sigma|^2$, where $\gamma_z = \sum_m m^2|\psi_m|^2$, $\eta = \sum_{m=-3}^{1}\sqrt{[12 - (m+2)(m+1)][12 - m(m+1)]}\,\psi_{m+2}^*\psi_m$, and $\sigma = \sum_{m=-3}^{2} m\sqrt{[12 - m(m+1)]}\psi_{m+1}^*\psi_m$. Removing spin-independent terms, the energy becomes $E = N\beta\epsilon/2$, with

$$\epsilon = \tilde{p}f_z + \tilde{c}_1 f_z^2 + \frac{4c_2}{7}|s_-|^2 + c_3\left(\frac{3\gamma_z^2}{2} - 12\gamma_z + \frac{|\eta|^2}{2} + 2|\sigma|^2\right), \quad (7)$$

where $\tilde{p} = 2p/N\beta$, and $\tilde{c}_1 = c_1 - c_3/2 + \sqrt{16\pi/5}\Gamma_0 c_d/\beta$. Since $c_d \ll c_1$, dipolar effects are not relevant for the equilibrium discussion. We will hence set $\Gamma_0 = 0$.

We have minimized Eq. (7) with respect to ψ_m, under the constraints $\sum_m|\psi_m|^2 = 1$ and $f_+ = 0$ [25]. Figure 1 shows the corresponding phase diagram, which although in basic agreement with that worked out recently in Ref. [22], presents small differences in its final form. For the phases discussed below $\sigma = 0$ [26]. For sufficiently negative g_0 the system is in a polar phase $P = (\mathbf{c}\theta, 0, 0, 0, 0, 0, \mathbf{s}\theta)$, with $\mathbf{c} \equiv \cos$, and $\mathbf{s} \equiv \sin$. This phase is characterized by $f_z \simeq -3\tilde{p}/\tilde{p}_c$ ($\tilde{p}_c \simeq 6\tilde{c}_1 \simeq 0.36$), $4|s_-|^2 = 1 - (\tilde{p}/\tilde{p}_c)^2$,

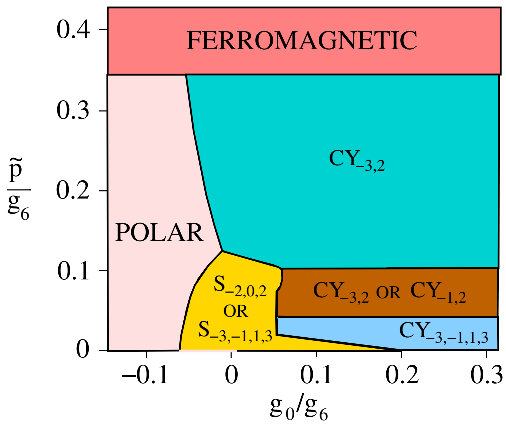

FIG. 1 (color online). Phase diagram function of g_0/g_6 and $\tilde{p}/g_6$, where $\tilde{p} = 2g_S\mu_B B/N\beta$.

$\gamma_z = 9$, and $|\eta| = 0$. The polar phase extends up to $g_0/g_6 = 0.01$ for $p = 0$ [27]. For sufficiently large g_0 and $\tilde{p}$, $CY_{-3,2} = (\mathbf{c}\theta, 0, 0, 0, 0, \mathbf{s}\theta, 0)$ occurs. This phase is cyclic ($s_- = 0$) and it is characterized by $f_z = -3\tilde{p}/\tilde{p}_c$, $\gamma_z \simeq 6 + 3\tilde{p}/\tilde{p}_c$, and $|\eta| = 0$. Both P and $CY_{-3,2}$ continuously transform at $\tilde{p} = \tilde{p}_c$ into a ferromagnetic phase $F = (1, 0, 0, 0, 0, 0, 0)$. For $0.04 < \tilde{p} \leq 2\tilde{c}_1 + 9c_3$ $CY_{-3,2}$ becomes degenerated with the cyclic phase $CY_{-1,2} = (0, 0, \mathbf{c}\theta, 0, 0, 0, \mathbf{s}\theta, 0)$. The latter state differs from $CY_{-3,2}$, since $\gamma_z = 2 - 3\tilde{p}/\tilde{p}_c$. For sufficiently large g_0 and $\tilde{p} < 0.04$, a cyclic phase ($CY_{-3,-1,1,3}$) of the form $(\psi_{-3}, 0, \psi_{-1}, 0, \psi_1, 0, \psi_{-3})$ occurs. Contrary to the other cyclic phases this phase is characterized by $|\eta| > 0$ [28]. Finally for a region around $g_0 = 0$ an additional phase with $|\eta| > 0$, $|s_-| > 0$ is found. In this phase two possible ground states are degenerated [29], namely $S_{-2,0,2} = (0, \psi_{-2}, 0, \psi_0, 0, \psi_{+2}, 0)$ and $S_{-3,-1,1,3}$, which has a similar form as $CY_{-3,-1,1,3}$.

For a Cr-BEC in a spherical trap of frequency ω in the Thomas-Fermi regime, $\tilde{p} = \tilde{p}_c$ for a magnetic field (in mG) $B \simeq 1.25(N/10^5)^{2/5}(\omega/10^3 \times 2\pi)^{6/5}$. Hence, most probably, magnetic shielding seems necessary for the observation of nonferromagnetic ground-state phases. We would like to stress as well that there are still uncertainties in the exact values of $a_{2,4,6}$. In this sense, we have checked for $a_6 = 98a_B$, $a_4 = 64a_B$, and $a_2 = -27a_B$, that apart from a shift of 0.2 towards larger values of g_0/g_6, the phase diagram remains qualitatively the same.

In the last part of this Letter, we consider the spinor dynamics within the MF approximation, but abandoning the SMA. The equations for the dynamics are obtained by deriving the MF Hamiltonian with respect to $\psi_m^*(\mathbf{r})$:

$$i\hbar\frac{\partial}{\partial t}\psi_m(\mathbf{r}) = \left[\frac{-\hbar^2\nabla^2}{2M} + U_{\rm trap} + pm\right]\psi_m + N[c_0 n + m(c_1 f_z + c_d\mathcal{A}_0)]\psi_m + \frac{N}{2}[c_1 f_- + 2c_d\mathcal{A}_-]S^+_{m,m-1}\psi_{m-1} + \frac{N}{2}[c_1 f_+ + 2c_d\mathcal{A}_+]S^-_{m,m+1}\psi_{m+1} + (-1)^m\frac{2Nc_2}{7}s_-\psi^*_{-m} + Nc_3\sum_n\sum_{i,j}O_{ij}(S^iS^j)_{mn}\psi_n, \tag{8}$$

where $\mathcal{A}_0 = \sqrt{6\pi/5}[\sqrt{8/3}\Gamma_{0,z} + \Gamma_{1,-} + \Gamma_{-1,+}]$, $\mathcal{A}_\pm = \sqrt{6\pi/5}[-\Gamma_{0,\pm}/\sqrt{6} \mp \Gamma_{\pm,z} + \Gamma_{\pm 2,\mp}]$, $\Gamma_{m,i} = \int d\mathbf{r}' f_i(\mathbf{r}')Y_{2m}(\mathbf{r} - \mathbf{r}')/|\mathbf{r} - \mathbf{r}'|^3$, and $S^\pm_{m,m\mp 1} = \sqrt{12 - m(m \mp 1)}$. Note that all ψ_m, n, f_i, O_{ij}, and $\mathcal{A}_i$ have now a spatial dependence. We first consider $p = 0$, and discuss on $p \neq 0$ below. There are two main features in the spinor dynamics in Cr-BEC which are absent (or negligible) in other spinor BECs. On one side the c_3 term allows for jumps in the spin manifold larger than 1, and hence for a rapid dynamics from, e.g., $m = 0$ to $m = \pm 3$. On the other side, the dipolar terms induce a EdH-like transfer of spin into c.m. angular momentum.

We consider for simplicity a quasi-2D BEC, i.e., a strong confinement in the z direction by a harmonic potential of frequency ω_z. Hence $\psi_m(\mathbf{r}) = \phi_0(z)\psi_m(\rho)$, where $\phi_0(z) = \exp[-z^2/2l_z^2]/\pi^{1/4}\sqrt{l_z}$, with $l_z = \sqrt{\hbar/m/\omega_z}$. We have then solved the 2D equations using Crank-Nicholson method, considering a harmonic confinement of frequency ω in the xy plane. In 2D, $\Gamma_{\pm 1,z} = 0$, but these terms vanish also in 3D due to symmetry, and hence the 2D physics is representative of the 3D one. The vanishing of $\Gamma_{\pm 1,z}$ is rather important, since if $\psi(t = 0) = \psi_{m=\pm 3}$, $\Gamma_{\pm 1,z}$ is responsible for a fast dipolar relaxation (for $\omega t \sim 1$). Hence, a BEC with $\psi(t = 0) = \psi_{\pm 3}$ does not present any significant fast spin dynamics. However, significant spin relaxation appears in the long time scale, due to the $\Gamma_{2,-}(\mathbf{r})$ terms. This is the case of Fig. 2, where we $\psi(t=0) = \psi_{m=-3}$ [30].

One of the most striking effects related with spin relaxation is the transference of spin into c.m. angular momentum, which resembles the famous EdH effect [23]. The analysis of this effect motivated us to avoid the SMA in the study of the spinor dynamics. In Fig. 2 we show snapshots of the spatial distribution of the $m = -2$ component. Observe that the wave function clearly loses its polar symmetry, since spin is converted into orbital angular momentum. The spatial patterns become progressively more complicated in time.

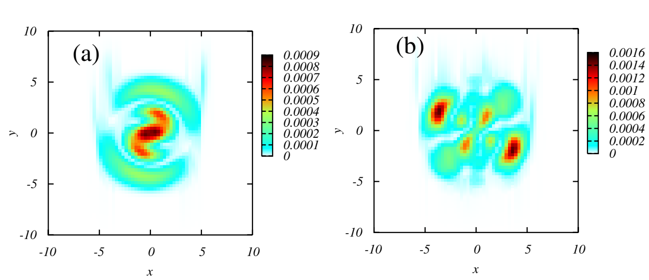

FIG. 2 (color online). $|\psi_{m=-2}(\mathbf{r})|^2$ at $\omega t = 40$ (a) and 120 (b) for $p = 0$, $g_0 = 0$, $\omega_z = 1$ kHz, $N = 10^4$ atoms, and $\psi(t = 0) = \psi_{m=-3}$. The x and y axes are in $\sqrt{\hbar/m\omega}$ units.

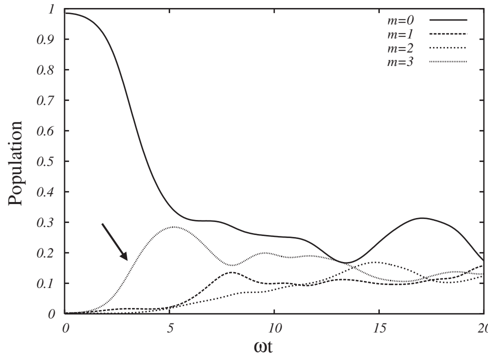

FIG. 3. Population of $\psi_{0,1,2,3}$ vs ωt for $g_0 = g_6$, $p = 0$, and $\psi(0) = \psi_0$. Note the rapid growth of $m = \pm 3$ (arrow).

The other special feature of Cr-BEC, namely, the appearance of the c_3 term, can have significant qualitative effects in the dynamics both for short and for long time scales. The evolution at long time scale may present interesting features, as large revivals, and it will be considered in future work. Here, we would like to focus on the short time scales, where the c_3 term may produce fast transference from $\psi_{m=0}$ to the extremes $\psi_{m=\pm 3}$. The latter is illustrated in Fig. 3, where we consider $g_0 = g_6$. The population is initially all in the $m = 0$ [30]. Contrary to the case of $F = 2$ in ^{87}Rb [12], there is at short time scales a jump to the extremes (the population of $\pm m$ is the same due to symmetry since $p = 0$). This large jump is absent if $c_3 = 0$, and depends on the value of g_0. In particular, if $g_0 = 0$ one obtains at short time scales a sequential population as for $F = 2$ ^{87}Rb [11].

We finally comment on the dynamics if $p \neq 0$. In the case of $F = 1$ or $F = 2$ ^{87}Rb, the dynamics is independent of p since the linear Zeeman effect may be gauged out by transforming $\psi_m \rightarrow \psi_m e^{ipmt/\hbar}$, due to the conservation of the total spin. In Cr-BEC the situation is very different, since the $\Gamma_{\pm 1,z}$ and $\Gamma_{\pm 2,\mp}$ do not conserve the total spin, and hence oscillate with the Larmor frequency $\omega_L = p/\hbar$ and $2\omega_L$, respectively. If ω_L is much larger than the chemical potential one may perform rotating-wave approximation and eliminate these terms. Hence the coherent EdH-like effect disappears for sufficiently large applied magnetic fields.

In conclusion, spin-3 Cr-BEC is predicted to show different types of spin phases depending on a_0 and the magnetic field. The spinor dynamics also presents novel features, as a fast transference between $\psi_0 \rightarrow \psi_{\pm 3}$, and the Einstein–de-Haas-like transformation of spin into rotation of the different components due to the dipole interaction.

We would like to thank M. Fattori for enlightening discussions, and the German Science Foundation (DFG) (SPP1116 and SFB/TR 21) for support. We thank H. Mäkelä and K.-A. Suominen for pointing us a mistake in previous calculations, and T.-L. Ho for enlightening email exchanges.

Note added in proof.—The EdH effect has also been recently discussed in Ref. [31].

[1] T.-L. Ho, Phys. Rev. Lett. **81**, 742 (1998).
[2] T. Ohmi and K. Machida, J. Phys. Soc. Jpn. **67**, 1822 (1998).
[3] C. K. Law, H. Pu, and N. P. Bigelow, Phys. Rev. Lett. **81**, 5257 (1998); H. Pu *et al.*, Phys. Rev. A **60**, 1463 (1999).
[4] C. V. Ciobanu, S.-K. Yip, and T.-L. Ho, Phys. Rev. A **61**, 033607 (2000).
[5] M. Koashi and M. Ueda, Phys. Rev. Lett. **84**, 1066 (2000); M. Ueda and M. Koashi, Phys. Rev. A **65**, 063602 (2002).
[6] H. Pu, W. Zhang, and P. Meystre, Phys. Rev. Lett. **87**, 140405 (2001).
[7] S. Yi, L. You, and H. Pu, Phys. Rev. Lett. **93**, 040403 (2004).
[8] T.-L. Ho and S. K. Yip, Phys. Rev. Lett. **84**, 4031 (2000); Ö. E. Müstercaplıoğlu *et al.*, Phys. Rev. A **68**, 063616 (2003).
[9] D. S. Hall *et al.*, Phys. Rev. Lett. **81**, 1539 (1998).
[10] J. Stenger *et al.*, Nature (London) **396**, 345 (1998).
[11] M. D. Barret, J. A. Sauer, and M. S. Chapman, Phys. Rev. Lett. **87**, 010404 (2001).
[12] H. Schmaljohann *et al.*, Phys. Rev. Lett. **92**, 040402 (2004).
[13] M.-S. Chang *et al.*, Phys. Rev. Lett. **92**, 140403 (2004); W. Zhang *et al.*, Phys. Rev. A **72**, 013602 (2005).
[14] T. Kuwamoto *et al.*, Phys. Rev. A **69**, 063604 (2004).
[15] M. H. Wheeler *et al.*, Phys. Rev. Lett. **93**, 170402 (2004).
[16] J. M. Higbie *et al.*, Phys. Rev. Lett. **95**, 050401 (2005).
[17] A. Widera *et al.*, Phys. Rev. Lett. **95**, 190405 (2005).
[18] N. N. Klausen, J. L. Bohn, and C. H. Green, Phys. Rev. A **64**, 053602 (2001).
[19] A. Griesmaier *et al.*, Phys. Rev. Lett. **94**, 160401 (2005).
[20] S. Yi and L. You, Phys. Rev. A **61**, 041604 (2000); K. Góral, K. Rzążewski, and T. Pfau, Phys. Rev. A **61**, 051601(R) (2000); L. Santos *et al.*, Phys. Rev. Lett. **85**, 1791 (2000); L. Santos, G. V. Shlyapnikov, and M. Lewenstein, Phys. Rev. Lett. **90**, 250403 (2003).
[21] J. Stuhler *et al.*, Phys. Rev. Lett. **95**, 150406 (2005).
[22] R. Diener and T.-L. Ho, this issue, Phys. Rev. Lett. **96**, 190405 (2006).
[23] A. Einstein and W. J. de Haas, Verhandl. Deut. Physik Ges. **17**, 152 (1915).
[24] J. Werner *et al.*, Phys. Rev. Lett. **94**, 183201 (2005).
[25] For every g_0 and $\tilde{p}$ we performed up to 2000 different runs of a simulated annealing method to avoid the numerous local minima.
[26] We also found numerically states [similar to the Z states of Ref. [22]] with tiny σ, which are however very slight variations of neighboring phases, with which they are in practice degenerated.
[27] For $p = 0$ we obtain the same results as in [22].
[28] $|\eta| \neq 0$ leads to the interesting possibility of biaxial nematics, as recently pointed out for the first time in Ref. [22].
[29] These phases are degenerated for any practical purposes, with relative energy differences $<0.01\%$.
[30] A small seed in the other components triggers the mean-field evolution.
[31] Y. Kawaguchi, H. Saito, and M. Ueda, Phys. Rev. Lett. **96**, 080405 (2006).